

## Thermal conductivity of solid H<sub>2</sub> in the orientationally ordered phase

Xiaoyu Li, David Clarkson, and Horst Meyer

*Department of Physics, Duke University, Durham, North Carolina 27706*

(Received 26 July 1990)

Simultaneous measurements of the thermal conductivity  $\kappa$ , the NMR line shape, and the thermal relaxation times  $\tau$  are reported for solid H<sub>2</sub> between  $0.4 < T < 2$  K and with ortho-H<sub>2</sub> concentrations  $0.5 < X < 0.7$ . From the NMR experiments, the second moment  $M_2$  (and hence the orientational-order parameter) was obtained. A combination of  $\tau$  and  $\kappa$  give a semiquantitative value for the specific heat  $C_p$ . In the long-range orientationally ordered (cubic) phase,  $\kappa$  is larger than in the disordered phase and for a given sample, we find  $d \ln \kappa / dX$  is nearly constant along isotherms. Extrapolation to pure *o*-H<sub>2</sub> suggests that  $\kappa(X=1)$  is of the same order as  $\kappa(X=0)$  for pure *p*-H<sub>2</sub>. A qualitative explanation is given for this enhancement in terms of the phonon scattering by the orientational excited states in the ordered phase. The observed anisotropy in  $\kappa$  in the cubic phase is discussed. We also have measured the boundaries and widths of the order-to-disorder transition in  $T$ - $X$  space as deduced mostly from determinations of  $\kappa$ ,  $M_2$ , and  $C_p$  as a function of  $X$  along isotherms. This width is attributed to inhomogeneities in  $X$ . The different profiles of the specific heat, depending on whether the transition is along isotherms or at constant  $X$ , are discussed. Sharp peaks in the conductivity are observed in the hcp phase of crystals having previously undergone order-disorder transition. The origin of these peaks is not understood.

### I. INTRODUCTION

So far, all the published measurements of the thermal conductivity  $\kappa$  of solid H<sub>2</sub> (Refs. 1–8) have been restricted to the hcp phase, where orientational ordering becomes short ranged with decreasing temperature. The reported measurements cover a wide domain for the ortho-H<sub>2</sub> (*o*-H<sub>2</sub>) concentration  $X$  and the temperature  $T$ . All experiments show that the highest thermal conductivity is observed for pure para-H<sub>2</sub> (*p*-H<sub>2</sub>), where the molecules are in the rotational ground state with angular momentum  $J=0$ . The introduction of *o*-H<sub>2</sub> impurities with  $J=1$  introduces an additional inelastic-phonon-scattering mechanism from the excitation of low-lying rotational states with energies  $\epsilon_i$  of the order of  $k_B T$ .<sup>9,10</sup> Observations<sup>1–8</sup> show that the resistivity  $\kappa_{o-H_2}^{-1}$  increases with  $X$  and with decreasing temperature.

Possibly these results have in the past discouraged measurements in the long-range ordered phase. Solid H<sub>2</sub> crystallizes in the hcp structure along the melting curve, and the transition into the ordered phase for  $X \geq 0.53$ , driven by intermolecular quadrupolar interaction, is accompanied by a crystalline phase change.<sup>11</sup> This transformation into a fcc lattice produces crystallites with different, though well-defined orientations,<sup>11</sup> and there is a large scattering of longitudinal and transverse sound.<sup>12</sup> One might then expect a low conductivity in the ordered phase of this inhomogeneous—but not randomly polycrystalline—medium. This anticipated low conductivity, combined with the heat generated through the ortho-para conversion, would then produce large temperature gradients across the sample as  $T$  decreases.

In this paper, we report the first measurements, to our knowledge, of  $\kappa$  in the ordered phase at various concen-

trations below  $X=0.7$ . Contrary to what might be expected on the basis of acoustic damping, the conductivity is larger in the ordered phase than in the short-range ordered or disordered hcp phase. At a given temperature,  $\kappa$  increases with  $X$ , and extrapolations to pure *o*-H<sub>2</sub>, indicate that  $\kappa$  might even become the same order as in *p*-H<sub>2</sub>. Thus, in the ordered state of pure *o*-H<sub>2</sub>, the inelastic phonon-scattering mechanism resulting from the excitation of librions with an energy  $\Delta$  much larger than  $k_B T$  is suppressed.

Our simultaneous measurements of  $\kappa$ , the NMR line shape, and the thermal relaxation time have permitted the correlation of the behavior of several properties in the region near the transition from orientational order to disorder. One of the results is the width in the  $T$ - $X$  plane over which both phases, the ordered and disordered, coexist. Hence, the predicted first-order transition is broadened. Although this spreading has been observed before,<sup>13–16</sup> it is presented here in more detail because of recent theoretical interest in crystallite formation and boundary effects during phase transformations.<sup>17</sup> Furthermore, there has been interest in the broadening of first-order transitions in solids with random quenched impurities,<sup>18</sup> for which the ortho-para-H<sub>2</sub> mixtures might be a good example.

The paper is organized as follows. In Sec. II, a brief review of conductivity experiments and theory in solid H<sub>2</sub> is given. Section III describes the experimental techniques and procedures, and, in Sec. IV, the results for the conductivity on ten samples from measurements as a function of  $T$  and from isothermal experiments as a function of time are presented. In Sec. V, the phase diagram and the boundaries of the coexistence region for the ordered and disordered phases are discussed in the light of measurements of  $\kappa$  and of NMR line shapes.

## II. BRIEF REVIEW OF PAST CONDUCTIVITY WORK

Measurements<sup>1-8</sup> include those on samples of nearly pure  $p$ -H<sub>2</sub>, with  $X < 0.03$ , as produced by catalytic conversion,<sup>1,2,7,8</sup> and with intermediate  $o$ -H<sub>2</sub> concentrations, up to  $X = 0.7$ .<sup>1,3,4,6</sup> Huebler and Bohn<sup>4</sup> and, later, Calkins and Meyer,<sup>6</sup> studied the conductivity of samples in the disordered (hcp) phase where the concentration, initially  $X \approx 0.75$  ("normal H<sub>2</sub>"), decayed over a period of time through ortho-para conversion. In this way, the effect of  $o$ -H<sub>2</sub> concentration on  $\kappa$  in a given sample could be systematically studied.

Recently, the effect of  $o$ -H<sub>2</sub> particle clustering on the conductivity, resulting from quantum diffusion, was studied<sup>7,8,10</sup> for  $X \leq 0.03$ . At larger concentrations, clustering will still take place, but the effect will be masked by the continuous conductivity change with time from ortho-para conversion.

The experiments all show very clearly that the addition of  $o$ -H<sub>2</sub> always decreases the thermal conductivity. Also, the maximum of  $\kappa$ , described via phonon scattering by the umklapp process, is decreased from its value for pure  $p$ -H<sub>2</sub> and shifted towards higher temperatures by the addition of  $o$ -H<sub>2</sub>.<sup>1,4</sup> Theory for  $\kappa$  (Refs. 5, 9, and 10) has been restricted to low concentrations and to high temperatures, where the energy states and the distribution of  $o$ -H<sub>2</sub> clusters (isolated  $o$ -H<sub>2</sub> singles and pairs in solid  $p$ -H<sub>2</sub>) can be calculated. The phonon-inelastic-scattering mechanism is from the excitation of the orientational states, determined principally by electric quadrupole-quadrupole interaction between the  $o$ -H<sub>2</sub> neighbors and also by the crystalline electric-field splittings.

One can write the inverse conductivity  $\kappa^{-1}$ , or thermal resistivity, as the sum from the terms expressing the phonon scattering by (1) the lattice, including defects, crystal boundaries, and umklapp processes, and (2) by the transition into higher orientational states via lattice-rotation coupling,

$$\kappa^{-1} = \kappa_{\text{lattice}}^{-1} + \kappa_{o\text{-H}_2}^{-1} \quad (1)$$

The first term is to be observed alone in solid para-H<sub>2</sub>, and the second term is introduced by the addition of ortho-H<sub>2</sub> with angular momentum  $J = 1$ . One can further write

$$\kappa_{\text{lattice}}^{-1} = \kappa_b^{-1} + \kappa_d^{-1} + \kappa_u^{-1} \quad (2)$$

where the terms represent phonon scattering by crystallite boundaries, defects, and umklapp processes. At sufficiently low temperatures, the first term dominates and is given by  $\kappa_b^{-1} = 3(C_v \nu \lambda_N)^{-1}$ , where  $C_v \propto T^3$  is the lattice specific heat per cm<sup>3</sup>. Also,  $\nu$  is the Debye velocity

$$\nu = \theta_D (k_B / h) (4\pi / 3\rho)^{1/3} \quad ,$$

$\rho$  is the number density of the crystal,  $h$  is Planck's constant, and  $\lambda_N$  is the temperature-independent mean free path between phonon collisions with the crystallite boundaries. Studies on carefully grown single crystals<sup>19</sup> of solid hcp <sup>4</sup>He show little anisotropy of this term. However, studies on <sup>4</sup>He assumed to be polycrystalline<sup>20</sup> showed

considerable influence of annealing on the magnitude of  $\lambda_N$ . (In <sup>4</sup>He crystals for  $T > 0.5$  K, a steeper increase of  $\kappa$  than  $T^3$ , characterizing Poiseuille flow, was observed.<sup>19</sup>) For H<sub>2</sub>, the contribution of the third term is observed in the region of 4 K, where  $\kappa_{\text{lattice}}$  passes over a maximum.<sup>1,4,7</sup>

The resistive term from the phonon scattering due to rotational states at temperatures above 1 K and for intermediate concentrations ( $0.2 \leq X < 0.72$ ) has been fitted<sup>4</sup> to an equation of the form

$$\kappa_{o\text{-H}_2}^{-1} = aX^2T^{-2} + bXT^{-3} \quad (3)$$

Results from experiments<sup>6</sup> between 0.2 and 1.5 K for this range of concentrations in the hcp phase have not been explicitly compared with this expression. They indicate an approximate form  $\kappa_{o\text{-H}_2}^{-1} \propto X^m T^{-n}$ , with  $2 < n < 3$  and  $m \approx 2$ .

At low concentrations ( $X \leq 0.03$ ), Kokshenev's theory<sup>10</sup> for temperatures above 1 K has successfully accounted for the conductivity experiments.<sup>2</sup>

## III. EXPERIMENTAL PROCEDURES

Our experiments, performed with the same apparatus as described in Ref. 6, used a conductivity cell with a sample diameter of 5 mm and length  $h = 2$  mm between parallel copper end pieces, where the contact surface was made of sintered copper to decrease the boundary resistance. Such a short sample length—contrasting with a length of 5 cm for experiments above 2 K (Refs. 1, 2, 4, and 7)—was necessary to reduce both the temperature difference  $\Delta T_{op}$  across the sample and the thermal relaxation time  $\tau$  at temperatures below 1 K. Here  $\Delta T_{op}$  results from the ortho-para conversion heat within the sample in the absence of an externally generated current. The time  $\tau$  is proportional to  $h^2 D_T^{-1}$ , where  $D_T$  is the thermal diffusivity. For the NMR experiment, a continuous-wave method using a Robinson low-level spectrometer was used, as previously described,<sup>15</sup> and the NMR line derivatives were recorded.

The fluid sample, having an initial concentration of  $X = 0.75$  was introduced into the cell as a pressure of  $\sim 110$  bars. During the crystallization along the melting curve, the supply capillary leading to the conductivity cell was heated intermittently so that the solid was formed at approximately constant pressure. The sample was then annealed close to the melting curve and slowly cooled to temperatures near 1 K over a period of 1–2 h. From previous research, the drop in pressure between the melting curve and 2 K was estimated to be approximately 40 bars.<sup>21</sup> From the known conversion rate,<sup>11</sup> the concentration was calculated as a function of time during the course of the experiments.

The decrease of  $X(o\text{-H}_2)$  with time prevented longer periods of annealing along the melting curve, and our growth technique gave, no doubt, less perfect samples than those obtained by Gorodilov *et al.*<sup>7</sup> NMR spectra taken on samples with  $X \approx 0.01$  showed a strong anisotropy when the field was applied in different directions.<sup>6,8</sup> Also, the NMR spectra taken on the samples in the orientationally ordered phase showed strong departures

from the spectra expected for polycrystalline material. They varied from one sample to another, reflecting different directions of crystal orientations because the spectra in the ordered phase are very anisotropic.<sup>15</sup> We conclude that our samples were not randomly polycrystalline.

Simultaneous measurements of the thermal conductivity, including the temperature equilibration process, and of the NMR line-shape derivative were carried out and stored in a computer. The thermal relaxation times were then determined from the temperature transients after the heat current was switched off. For  $t \geq \tau$ , these transients decayed as  $e^{-t/\tau}$ , where  $t=0$  marks the time of the interruption in the heat current. The measured relaxation times covered a range between 4 and 35 sec. In Fig. 1, we show two representative transients on a semilogarithmic scale for a "short" and a "long" time  $\tau$ . The vertical scale is the normalized amplitude  $\delta T(t)/\Delta T$ , where  $\delta T(t)$  is the temperature difference across the H<sub>2</sub> sample and  $\Delta T = \delta T(t=0)$  is the temperature difference at  $t=0$  when the heat current is cut off. It can be seen that the decay is exponential for  $\delta T(t)/\Delta T < 0.7$ . From a fit to the data,  $\tau$  is determined to within  $\sim 5\%$ .

The relaxation times were used to obtain a heat capacity signature in the transition region. For a flat sample with height  $h$  much smaller than its width, assuming  $C_p \simeq C_v$ , the slowest mode has a relaxation time given by

$$\tau_0 = \left( \frac{2h}{\pi} \right)^2 C_p / \kappa, \quad (4)$$

where  $C_p$  is the specific heat per cm<sup>3</sup>. In our cell, where the width is comparable with the height, this relation is only approximate, and we also expect an additional contribution to  $\tau$  from the heat capacity of the cell bottom part (see Fig. 1 in Ref. 6). Nevertheless, we can expect that, for given experimental values of  $\kappa$  and  $\tau$ , the heat capacity of the H<sub>2</sub> sample is qualitatively given by  $C_p = \text{const} \times (\kappa\tau)$ . This relation is valid provided that we can neglect the heat capacity of the cell in comparison with that of solid H<sub>2</sub>. Numerical estimations show this condition to be realized below  $\sim 1$  K.

Two different procedures were followed for the con-

ductivity and line-shape measurements. In the first, the sample was cooled through the transition to  $T=0.4$  K following the crystallization and annealing. Data taking then proceeded as a function of temperature, until 0.2 K above the transition, which was determined from the sharp drop of the conductivity and of  $M_2$ . The sample was then cooled again to 0.4 K, and a new series of measurements was started. Generally, three such series were carried out, with the first one beginning with  $X \simeq 0.70$  and the last one ending as the concentration had decayed to  $X \simeq 0.55$  after 20 h. Finally, the sample was cooled again to 0.4 K but was no longer in the ordered phase, because  $X$  was below the limiting value  $X \simeq 0.53$ . A series of measurements with  $X=0.51$  were then taken as a function of  $T$  up to 2.0 K. Their purpose was to obtain  $\kappa(T)$  to serve as a comparison with similar measurements at 0.51 on other samples all crystallized with the same annealing procedure.

In the second procedure, the sample was cooled through the transition to a temperature  $T$  in the range between 0.4 and 1.2 K, and measurements were then taken quasi-isothermally, where the temperature of the colder end was kept constant by servoregulation. The average sample temperature decreased slightly as a function of time because of the decrease in the conversion-generated heat. The measuring procedure, both for  $\kappa$  and for the NMR line shape, was entirely automated and clearly showed the transition region by a change in the NMR line shape, conductivity, and equilibration time. When the concentration of  $X \simeq 0.51$  was reached, the sample was cooled to 0.4 K, and a control series of conductivity data as a function of  $T$  up to 2.0 K was started, as described before. Twelve such isothermal experiments were carried out at regular temperature intervals.

To evaluate the conductivity measurements, corrections necessitated by the ortho-para (*op*) conversion heat had to be made, as already described in Ref. 6. For instance, for  $X=0.7$ , in the absence of external heat, the temperature difference at  $T=0.4$  K between the cold and the warm end plates was  $\Delta T_{op} = 0.025$  K. As  $X$  decreased through ortho-para conversion, this difference increased only slightly with time in the cubic phase because of two effects working in opposite directions. These are

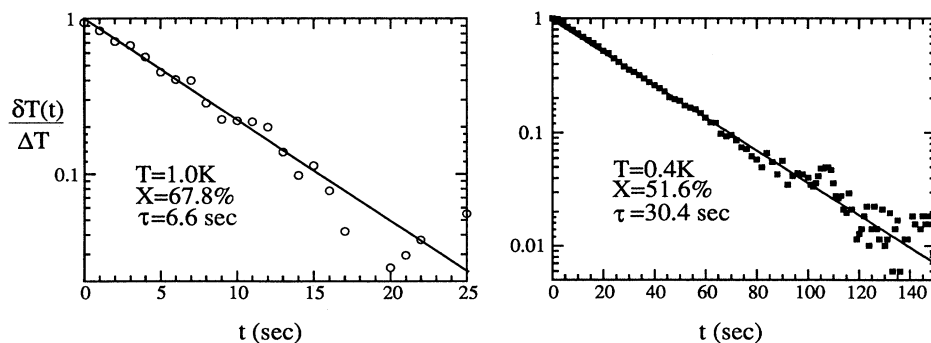


FIG. 1. Two representative normalized decays of the temperature difference  $\delta T(t)$  across the solid H<sub>2</sub> sample after the heat current is turned off at  $t=0$ . Here  $\Delta T = \delta T(t=0)$ . The relaxation time is obtained from a fit of an exponential to the data (solid line).

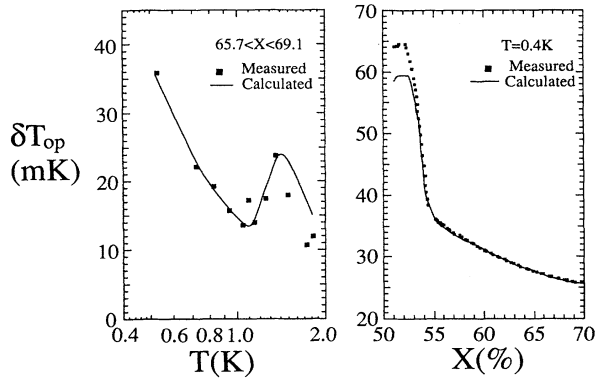


FIG. 2. The difference in temperature  $\Delta T_{op} = T_{hot} - T_{cold}$  between the extremities of the sample of length  $l = 2$  mm, produced by self-heating through ortho-para (*op*) conversion. (a) As a function of temperature with  $0.67 < X < 0.7$ , and (b) as a function of  $X$  along the isotherm  $T = 0.4$  K. The solid lines are calculated as explained in the text.

the decrease in the conversion rate and in the conductivity as  $X$  decreases. At the transition into the disordered hcp phase, where  $\kappa$  was found to decrease,  $\Delta T_{op}$  showed a steep rise. In Fig. 2, we show this temperature difference, induced by *op* conversion, both as a function of  $T$  and of  $X$ . The solid lines are calculations that use the heat of conversion (from the known conversion energy and rate), the cell dimensions, and the measured conductivity of solid  $H_2$ . Hence, the temperature drop is quantitatively understood.

## IV. RESULTS AND DISCUSSIONS

### A. Overview of the simultaneous data

The main purpose in carrying out simultaneous measurements of three properties, namely, the conductivity, the NMR line shape, and the relaxation time leading to an estimate of the  $C_p$ , was to establish their correlation in the region of the transition. It was desirable to find out

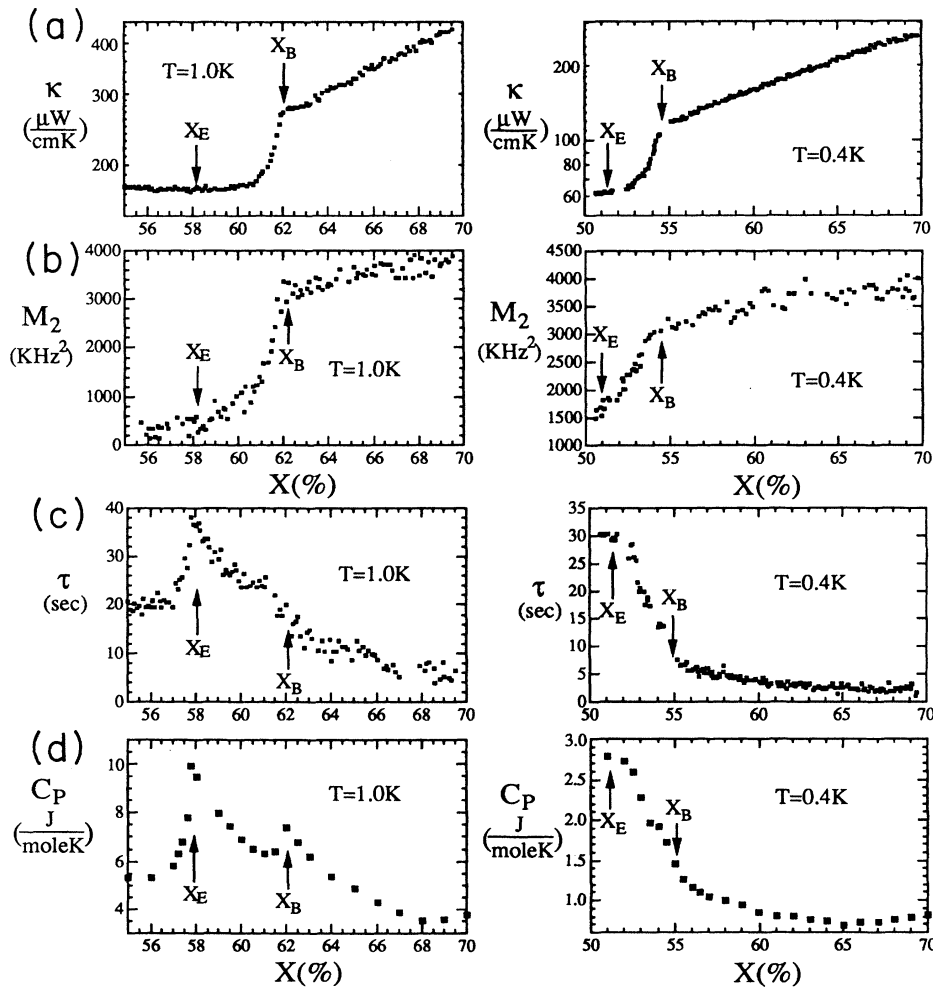


FIG. 3. Measurements (a) of the conductivity  $\kappa$ , (b) the second moment  $M_2$ , and (c) the relaxation time  $\tau$  along the isotherms  $T = 1.0$  K (left-hand side) and  $0.4$  K (right-hand side). From a combination of smoothed data of  $\kappa$  and  $\tau$  via Eq. (6), the specific heat is presented in (d). The arrows with  $X_B$  and  $X_E$  mark the beginning and the end of the coexistence region.

how and when each measurement detected the beginning and the end of the phase change. In Fig. 3, the left-hand side shows an example of an isothermal run at 1.0 K, which is representative for the "high-temperature" regime. The experiment started at  $X=0.7$  and was terminated at  $X=0.55$ . Figure 3(a) shows the conductivity, which drops more sharply below  $X=0.62$  and is roughly constant for  $X \leq 0.58$ . By two vertical arrows we mark the sharply defined beginning ( $B$ ) and the poorly defined ending ( $E$ ) of the phase transformation at  $X_B$  and  $X_E$ . The latter concentration was estimated by noting that a plot of  $\log \kappa$  versus  $X$  for  $X \geq 0.45$  for various isotherms in the hcp phase gave a straight line with zero or a slightly negative slope. The concentration range, where the data started to depart upward from the straight line, was taken as  $X_E$ . Figure 3(b) presents the partial second moment,  $M_2$ , corresponding to sweep over a frequency range of  $\pm 130$  kHz from the line center. Hence, this sweep does not include the outer "wings" of the whole line structure,<sup>15</sup> the intensity of which is small compared with the main doublet. Since the main interest was in the phase change, as recorded by the NMR line shape, we decided not to record the outer wings. We note, again by arrows, what we perceive to be the beginning  $X_B$  and the ending  $X_E$  of the transition, and where  $X_B - X_E \approx 4\%$ . For the determination of  $X_E$ , less sharply defined than  $X_B$ , we use the same argument as in Fig. 3(a), namely, that  $M_2$  versus  $X$  is found to be roughly linear along an isotherm in the hcp phase for  $X \geq 0.45$ . Figure 3(c) presents the relaxation time with no well-defined beginning of the transition but with a sharp peak at the end. Finally, Fig. 3(d) shows the specific heat, obtained by combining the  $\tau$  and  $\kappa$  data via Eq. (6). Because of the uncertainties in the calculation of  $C_p$ , we only give qualitative significance to the results in Fig. 3(d), which carries

the interesting signature of two peaks, again pinpointed by two vertical arrows. We note that the location of  $X_B$  and  $X_E$  in Figs. 3(a), 3(b), and 3(d), done separately, is internally consistent within the uncertainties.

On the right-hand side of Fig. 3, we show in similar fashion a representative run in the "low-temperature" regime at  $T=0.4$  K. Here the conductivity shows a behavior analogous to that at 1.0 K, with the transition shifted to lower  $X$ . Here  $M_2$  shows only a well-defined beginning at  $X_B$  but no sharp ending. At what we label  $X_B$ ,  $\tau$  starts to rise sharply with decreasing  $X$  and tends to a plateau at what we presume to be the end of the transition,  $X_E$ . The specific heat shows a smooth behavior and no longer the presence of two peaks. Experiments at temperatures between 0.4 and 1.0 K show a continuous change from one to the other extreme. Again, the location of  $X_B$  and  $X_E$  from the various experiments is internally consistent.

In Fig. 4, we show measurements as a function of  $T$ . During the time needed to warm the sample from 0.43 to 1.8 K, the ortho concentration decayed from  $X=0.653$  to 0.624. In Fig. 4(a), the transition beginning follows a broad maximum in the conductivity, but the end is sharp. Figure 4(b) shows the second moment with its sharp decrease above 1.1 K beginning and ending of the phase transition at  $T_B$  and  $T_E$ . The sharp maximum of the relaxation time and of the heat capacity is located at  $T=1.15$  K. We mark the beginning and the end of the singularity by two arrows with  $T_B$  and  $T_E$ . Contrary to the measurements along isotherm  $T=1.0$  and also 1.2 K (not shown), the heat capacity has only one peak when the sample is heated through the transition. This peak is located at a temperature between  $T_B$  and  $T_E$  as determined from  $\kappa$  and  $M_2$  data.

The information shown so far leads to the conclusion that, for a given route, the location of the transition be-

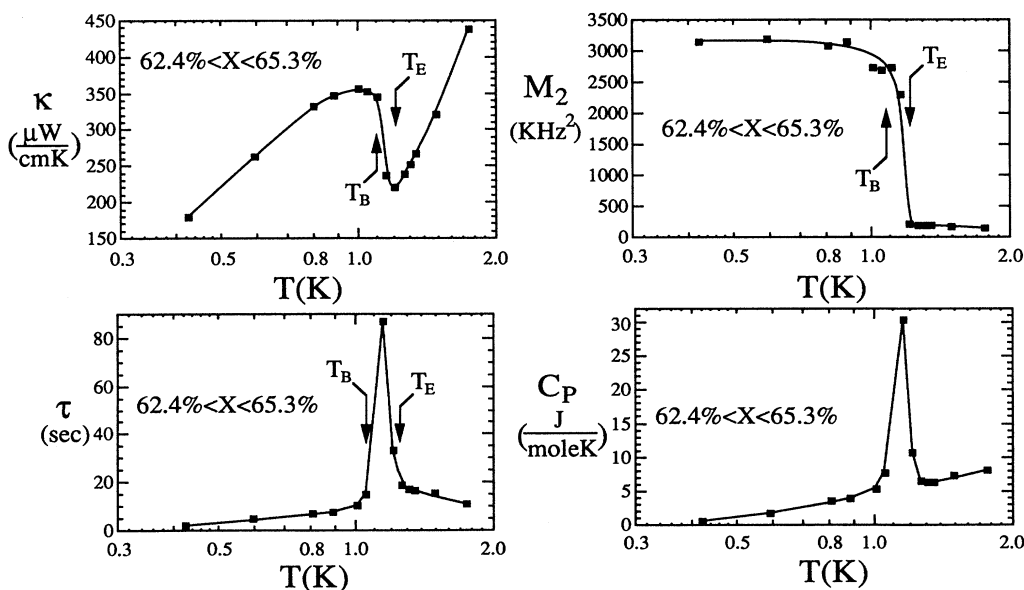


FIG. 4. Same display of measurements as in Fig. 3 but as a function of  $T$ , at nearly constant  $X$ .

gining and end are quite well defined. In what follows, we examine each property separately and then discuss the transition location and its width, as determined both from isotherms and from temperature sweeps.

### B. Thermal conductivity

First, we show in Fig. 5, a global survey of data (a) for  $X \approx 0.70$ , which show the transition to the ordered phase, (b) for  $X \approx 0.50$ , where  $H_2$  remains in the hcp phase with short-range order at sufficiently low temperatures, and finally (c) for  $X \sim 0$ , where the conductivity is highest because there is no phonon scattering from orientational excitations. These data are a compendium of those taken by Huebeler and Bohn<sup>4</sup> (see their Figs. 2 and 3) at temperatures above 4 K, those obtained in a recent work<sup>8</sup> for  $X \approx 0$ , and, finally, those reported in this paper where the same cell was used as in Ref. 8. The maximum in  $\kappa$  near 9 K is related to the umklapp processes in the disordered phase, while that near 1 K marks the order-to-disorder transition. The dashed lines joining the two sets of data represent interpolations and the two maxima are well separated. This is in contrast to the situation with other materials showing ordering transitions, such as  $KH_2PO_4$ -type dielectrics, where one single maximum is observed.<sup>22</sup>

The situation in solid  $N_2$  is similar to that in  $H_2$ , as there is also a transition (from a disordered  $\beta$  phase, hcp, to an ordered  $\alpha$  phase, fcc), which is related to the orientational order-disorder transition of the  $^{14}N_2$  quadrupolar moments.<sup>23</sup> There is a sharp increase in the conductivity<sup>24</sup> as  $T$  is decreased below the transition, similarly to  $H_2$  and to the ferroelectrics. However, the maximum in  $\kappa$  for  $N_2$  has not yet been reported, as measurements<sup>24</sup> do not extend below 5 K.

Second, we briefly show evidence in Fig. 6(a) of a strong apparent conductivity anisotropy in the ordered phase. When plotted versus  $T$ , the conductivity data at composition  $X=0.7$  for nine samples along different isotherm (crosses) appear to fall into two classes, one with a

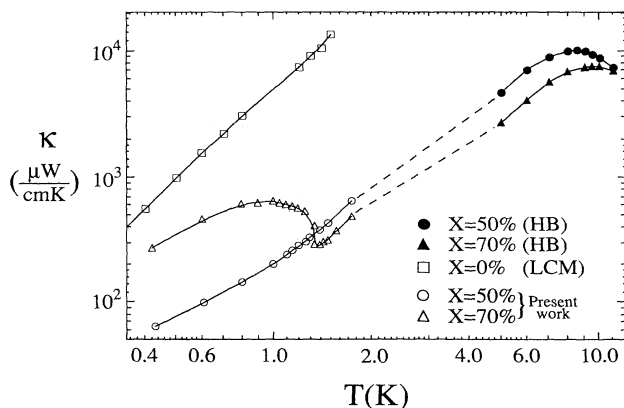


FIG. 5. Thermal conductivity data for  $X=0.7$ ,  $0.5$ , and  $\sim 0$  between  $0.4$  and  $12$  K. Data for  $4 < T < 12$  K are from Ref. 4. Data for  $X=0$  are from Ref. 8; data for  $X=0.7$  and  $0.5$  for  $T < 2$  K are from the present work.

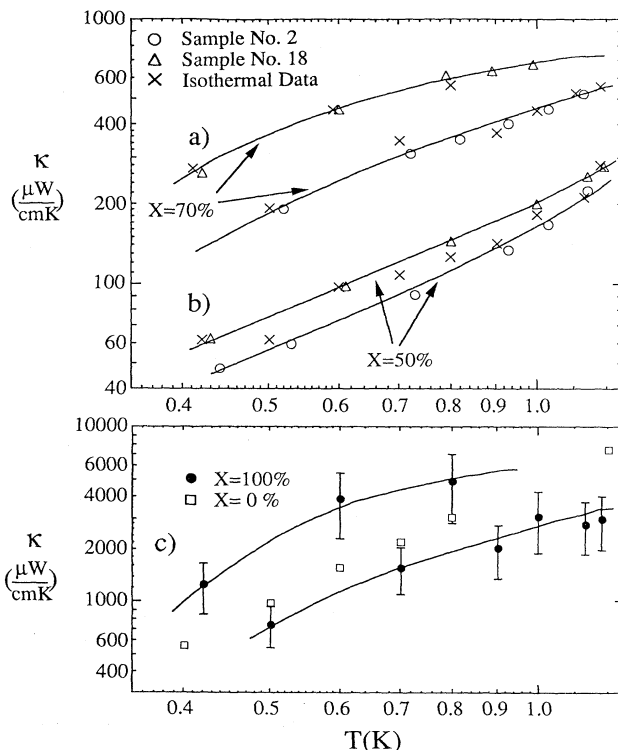


FIG. 6. The conductivity for (a)  $X=0.7$  and (b)  $X=0.5$  from nine isotherms and comparison with experiments at constant  $X$  vs  $T$  (samples Nos. 2 and 18). In (c), the extrapolated conductivity for  $X=1$  is shown by solid circles. The open squares are results for  $X=0$ . The solid lines are a guide to the eye for the high and the low conductivity crystal orientation.

“higher” and one with a “lower” conductivity. This is illustrated by a plot of the data for  $\kappa$  versus  $T$  for two samples (Nos. 2 and 18) with  $X \approx 0.70$  (open circles and triangles). The solid lines are a guide to the eye through the data points.

One might suspect at first that the difference is caused by the quality of the samples and by imperfect bonding to the copper end pieces. However, the observation of only two “classes” in the  $\kappa$ -versus- $T$  plot seems to indicate that this explanation might not be correct, since it leads one to expect various intermediate degrees of crystal quality and bonding strengths. This would give a scatter in a  $\kappa$ -versus- $T$  plot instead of two lines of points. Moreover, according to our estimations, the pressure in the cell was always larger than  $\sim 70$  bars, so the bonding to the surface should always have been strong. It thus appears that, in our cell, there are two preferential directions of crystallization resulting in a substantial anisotropy of the thermal conductivity in the ordered phase. By contrast, the anisotropy is less pronounced in the hcp (short-range-ordered) phase, as shown in Fig. 6(b) for  $X \approx 0.50$ . Here again we present, using the same symbols as above, the data from isotherms for nine samples and those from  $\kappa$ -versus- $T$  measurements on sample Nos. 2 and 18.

Although the conductivity anisotropy in the cubic phase is totally unexpected, it should be remembered that

the sample is not a homogeneous single crystal but, rather, an assembly of cubic domains with well-defined orientations, separated by domain walls that are likely to be hcp. Hence, this large observed anisotropy is not an intrinsic property but is indicative that the medium is not truly cubic.

We further note that for each isotherm, with representative examples shown in Fig. 3, the slope  $d \ln \kappa / dx$  in the ordered phase is nearly constant for each sample. This suggests an admittedly bold linear extrapolation on such a plot to  $X=1$  (pure *o*-H<sub>2</sub>), and the results are shown in Fig. 6(c). Here again, the higher and lower conductivity regions appear, and the solid lines are again drawn as a guide to the eye. Comparison with the data of pure *p*-H<sub>2</sub> (open squares) and measured with the same cell, suggests that  $\kappa$  in the ordered phase is roughly the same as in *p*-H<sub>2</sub>. Hence, the scattering of phonons by orientational excitations is small for  $X=1$  but increases with dilution by *p*-H<sub>2</sub>. This can be explained qualitatively as follows: In the ordered phase, the orientational ground state for *o*-H<sub>2</sub> is separated from the first excited state of the “librons” by an energy gap  $\Delta$  that, for pure *o*-H<sub>2</sub>, is  $\Delta/k_B \approx 16$  K.<sup>25,26</sup> Hence,  $\Delta \gg k_B T$  and the librons cannot be excited by phonon scattering. But with the addition of *p*-H<sub>2</sub> impurities, the gap decreases and becomes progressively replaced by a more complex structure of energy states. With decreasing  $X$ , the width of this structure becomes comparable with  $k_B T$ , thus leading to increased phonon scattering by the orientational excited states in the cubic ordered state. Finally, the scattering will be comparable with that in the short-range ordered state.

The larger anisotropy for  $\kappa(X=1)$  than for  $\kappa(X=0.70)$  in the cubic phase might well be due to the uncertainties in the extrapolation to  $X=1$ . Inspection of  $\kappa$  for the three isotherms ( $T=0.42, 0.60,$  and  $0.80$  K) giving the higher conductivity shows a slight but steady decrease of the slope  $d \ln \kappa / dX$  with increasing  $X$ . Hence, the linear

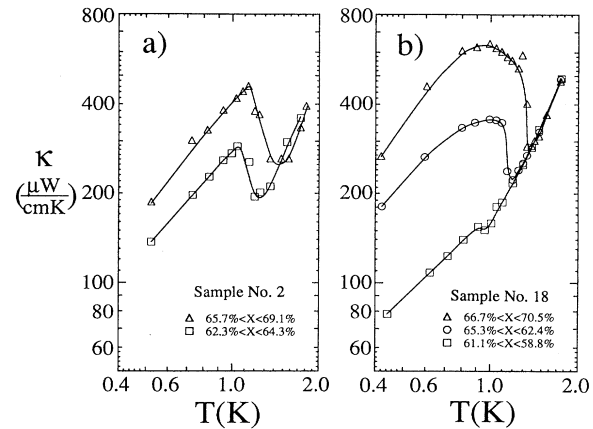


FIG. 7. Thermal conductivity vs  $T$  for several experiments on two samples Nos. 2 and 18, showing systematic differences in the shape  $\kappa(T)$  at temperatures near the transition.

extrapolation made for the plot in Fig. 6(c) very possibly gives too high values of  $\kappa$  for these isotherms. By contrast, the isotherms with lower conductivity do not show this slight flattening off, and it is not excluded that there is even an increase in the slope  $d \ln \kappa / dX$  at higher  $X$ . Hence, the anisotropy of  $\kappa$  for  $X=1$  might well be smaller than indicated by the simple crude linear extrapolation. Again we point out that the observed anisotropy in the cubic phase is not intrinsic to a cubic crystal but must be attributed to the inhomogeneous nature of the sample below the martensitic transition.

We now present in Fig. 7 two sets of conductivity results versus  $T$  on two samples showing a different behavior close to the transition. In both samples, the effect of the ortho concentration on  $\kappa$  is very striking. The steep

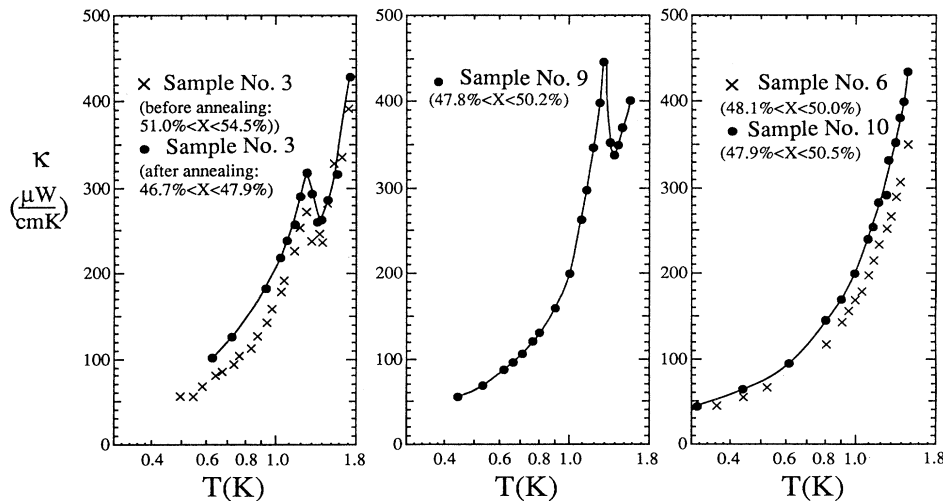


FIG. 8. Thermal conductivity in the hcp (disordered) phase at  $X \approx 0.5$  after the sample has undergone two or more passages through the order-disorder transition at higher ortho concentrations. (a) and (b) show samples where an anomalous peak was detected, without and with annealing. (c) Shows two samples without such anomaly.

TABLE I. List of various samples used in the investigations, their route through the order-disorder transition, and the presence (or lack) of a peak in  $\kappa$  near  $T \cong 1.4$  K after completing the transition experiments.

| Sample | Route                      | Peak amplitude in hcp phase ( $\mu\text{W}/\text{cmK}$ ) |
|--------|----------------------------|--|
| 1      | vs $T$ (three passes)      | 0  |
| 2      | vs $T$ (four passes)       | 30   |
| 3      | isothermal $T = 1.13$      | 60   |
| 4      | vs $T$                     | 0  |
| 5      | vs $T$ (two passes in hcp) | 10   |
| 7      | $T = 100$ K                | 40   |
| 8      | 0.8 K                      | 0  |
| 9      | 0.7 K                      | 150  |
| 10     | 0.6 K                      | 0  |
| 11     | 0.5 K                      | 0  |
| 12     | 0.42 K                     | 0  |
| 13     | 0.42 K                     |  |
| 14     | 0.51 K                     | 50   |
| 15     | 0.8 K                      | 0  |
| 16     | $T = 0.9$ K                | 0  |
| 17     | $T = 1.18$ K               | 125  |
| 18     | vs $T$ (three passes)      | 0  |

increase of  $\kappa$  with  $T$  in the short-range ordered phase progressively reduces the visibility of the transition as  $X$  decreases. The first sample in Fig. 7(a) shows a sharply peaked conductivity near the transition for both series of measurements. The second sample, Fig. 7(b), by contrast shows a much broader maximum. We do not understand the reason for these differences.

Another puzzling observation is that of a conductivity anomaly in the short-range ordered phase, recorded with several samples that had previously been cooled into the

cubic ordered phase, while the ortho concentration was higher than  $X = 0.6$ . This anomaly was observed as a sharp peak in the range of 1.3–1.4 K. Figure 8(a) shows by crosses and solid circles the results before and after a 2-h annealing period near the melting curve. Figure 8(b) shows an example of a still larger anomaly at  $T = 1.3$  K for another sample. Finally, Fig. 8(c) shows results for a third and fourth sample with no anomaly at all. Samples never cycled through the transition did not show the anomaly either. By a curious and intriguing coincidence, the samples that have shown a “large” conductivity in the ordered phase do not evidence such a sharp maximum in  $\kappa$  after the ortho concentration decayed to for  $X \cong 0.5$ . However, those crystallized in a direction to give a “low”  $\kappa$  in the ordered phase show the maximum. In Table I, we summarize our results with the various samples and give an estimate for the amplitude of the anomalous peak.

### C. The NMR line shape

It has been known for many years<sup>13,15</sup> that upon warming an orientationally ordered  $\text{H}_2$  sample towards the transition, the NMR line shape starts changing continuously over a temperature range of roughly 0.1 K below the transition. Figure 9(a) shows a series of integrated line shapes for  $X \approx 0.68$  taken with increasing  $T$ . Only one-half of the symmetric lines are shown, and they are vertically displaced to avoid overlapping. In the top spectrum, for  $T \leq 1.25$  K one notes the doublet structure at  $\pm 75$  kHz, characteristic of the ordered state, and a broad maximum at the center. This maximum has been found previously to be absent for polycrystalline samples,<sup>13</sup> but it is present in samples grown as hcp single crystals and is in agreement with predictions.<sup>15</sup> It is not a sign of orientational disorder. In Fig. 9(a), at 1.3 K, this maximum becomes slightly enhanced, but more so as  $T$

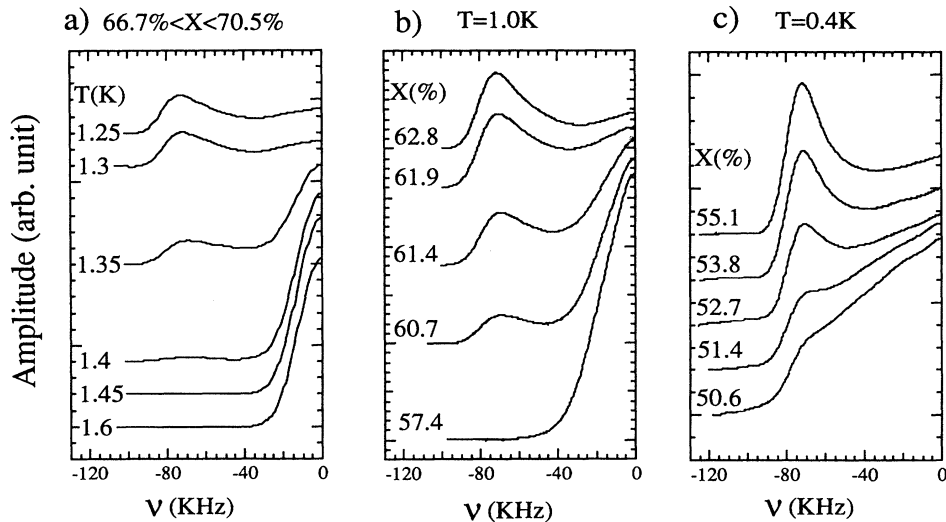


FIG. 9. The left half of the symmetric NMR line for  $\text{H}_2$  in the region near the transition (a) with increasing  $T$ , at nearly constant  $X \approx 0.68$ . (b) With decreasing  $X$  along the isotherm  $T = 1.0$  K. (c) As in (b) but for  $T = 0.4$  K.

increases. The doublet structure intensity decreases and the temperature where it disappears,  $T \approx 1.45$  K, had been previously<sup>13</sup> labeled as the transition point. No particular attention had been paid to the coexistence of disordered and ordered phases represented by the sharp center line and the doublet structure, respectively, as the transition was believed to be first order. The width  $\Delta T \approx 0.15$  K, is detected regardless of whether the crystal is at zero pressure, where its density can change at the transition, or whether it has been grown under pressure, where the order-disorder transition takes place at constant density.

Figure 9(b) shows the transition along an isothermal run at  $T = 1.0$  K, and the spectrum change with decreasing  $X$  is very similar to that in Fig. 9(a). For  $X = 0.574$ , the doublet structure has disappeared. Both Figs. 9(a) and 9(b) describe transitions in neighboring regions of the  $T$ - $X$  phase diagram.

By contrast, Fig. 9(c) shows a run along the isotherm  $T = 0.4$  K. Although the doublet structure disappears, the structure around the center is much broader than at 1.0 K, reflecting substantial short-range order. The difference between the NMR spectra of long-range and short-range orders near the transition is still smaller at lower temperatures, as previous measurements have shown (see Figs. 1 and 4 in Ref. 27). We conclude from the evidence shown in Figs. 9(a), 9(b), and 9(c) that, at the transition, the disordered and the long-range ordered phases coexist over a certain width in  $T$ - $X$  space, which will be discussed in more detail in Sec. IV D. Hence, the argument for a simple first-order phase transition in H<sub>2</sub> needs to be modified in favor of a more complex transition type.

The situation in solid D<sub>2</sub> is similar and is particularly illuminating because here the order-disorder transition can be made to take place with or without a crystalline

(cubic-to-hcp) phase change. After repeated thermal cyclings through the transition, the cubic phase becomes stabilized even above the transition as shown by a variety of experiments.<sup>11</sup> (In solid H<sub>2</sub>, this state cannot be achieved, and the disordered phase is always hcp.) Inspection of D<sub>2</sub> NMR line shapes<sup>28,29</sup> indicates clearly a region where the ordered and disordered phases coexist. This phenomenon takes place with and without stabilization of the cubic crystalline phase above the transition by repeated thermal cyclings. In Fig. 10, we show the NMR spectrum in D<sub>2</sub> through the transition, without and with stabilization of the cubic phase.<sup>29</sup> We conclude, that, since the phase coexistence region exists in the cycled condition where there is no martensitic transition, its width cannot be caused principally by the crystallographic changes. Hence, we will assume that the same might be true in solid H<sub>2</sub>.

#### D. The specific heat

Our measurements of  $\tau$  and  $\kappa$  do not give a quantitative measurement of  $C_p$  of H<sub>2</sub> because our analysis is oversimplified in view of the sample geometry. Nevertheless, they show some striking features that are different during transitions along isotherms and at nearly constant  $X$ . Figure 11 shows the signature of  $C_p$  along these two routes, where the various curves have been shifted both vertically to avoid overlapping and also horizontally to make the transition regions coincide. The dashed horizontal areas at the bottom of Figs. 11(a) and 11(b) show the region of coexistence.

In the high-temperature regime, namely, for  $T > 0.9$  K, the transition along an isotherm is highlighted by two peaks, the largest of which is near the completion of the transition. This is different from the conductivity change

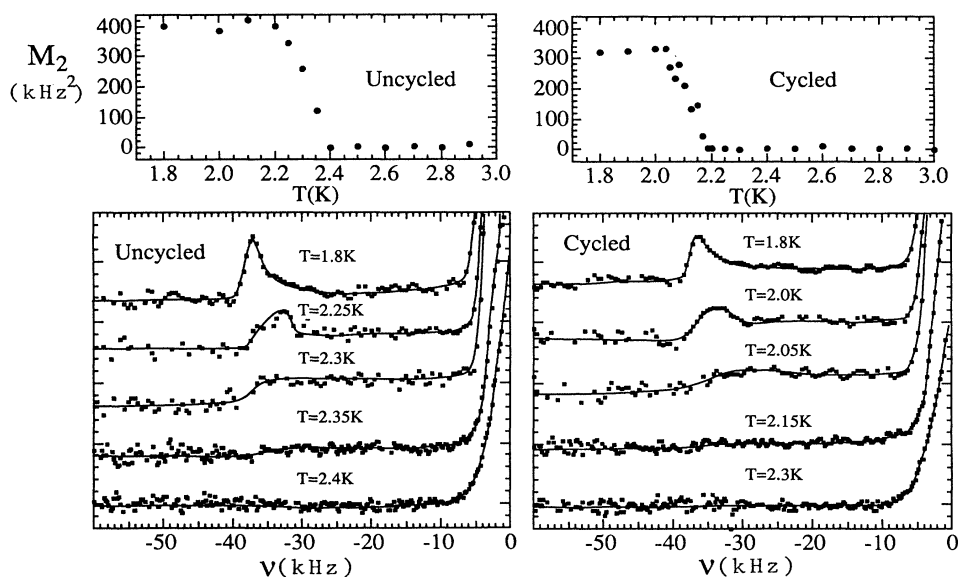


FIG. 10. The left half of the symmetric NMR line for D<sub>2</sub> in the region near the order-disorder transition with increasing temperature. Left-hand side, before, and right-hand side, after, stabilization of the cubic crystalline phase by repeated thermal cyclings.

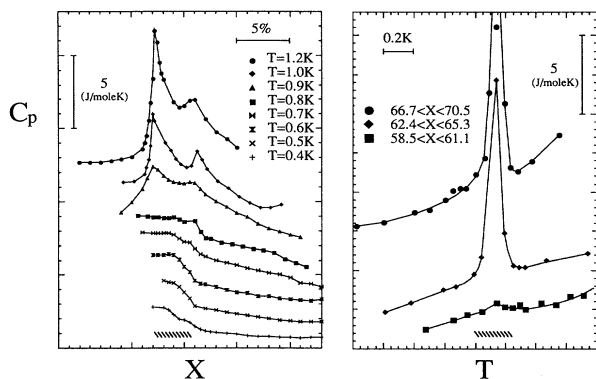


FIG. 11. The specific heat obtained from relaxation time and conductivity measurements as the order-to-disorder transition progresses. (a) along several isotherms with decreasing  $X$ , and (b) at constant  $X$  with increasing  $T$ . The vertical and horizontal scales are explained in the text. The dashed marks at the bottom of the figure indicate the transition width in  $X$  and in  $T$ , respectively.

(see Fig. 3), which is the steepest at the beginning of the transition and very small near the end. As  $T$  decreases, the small peak disappears and the completion of the transition is seen from the broad maximum of  $C_p$ . The specific heat, measured versus  $T$  at nearly constant  $X$ , only displays one peak, situated in the middle of the transition, the intensity of which decreases as  $X$  decreases.

It is puzzling why there is only one peak for the transition versus  $T$  at high  $X$ , while for the isothermal transition in a comparable region of the  $X$ - $T$  phase diagram there are two peaks. Perhaps this is due to the different ways the respective measurements were carried out. The experimentation time and, hence, the number of data points for the transition recorded as a function of  $T$  at nearly constant  $X$  was limited by the ortho-para conversion. There may have been possible equilibration problems close to and within the transition, leading to a collapsing of the two peaks into one. By contrast, the isotherm measurements were carried out under much better equilibration conditions, where many more measurements could be taken and, hence, the peak resolution was much better.

The specific-heat measurements of Ahlers and Ortung<sup>30</sup> also showed the existence of structure in the transition. Commonly, but not always, two or three peaks were observed, but where the maximum at the lowest temperature (i.e., at the transition beginning) was always the largest. This is in contrast with our experiments, where the largest peak appears at the end of the transition. The width of the structure was of the order of 0.15 K for  $X=0.72$ . (See Figs. 3–6 in Ref. 30.) These results were obtained by letting the sample, previously cooled below the transition, warm up via the ortho-para conversion heat. The temperature was recorded as a function of time, which led to the determination of the specific heat. These measurements were probably done under comparable equilibration conditions to our conductivity experiments along isotherms.

### E. The phase coexistence region

In Fig. 12, we show the phase diagram for the orientational long-range-to-short-range order transition. The two curves presented in Fig. 12 should not be confused with those expressing the hysteresis in the transition from the hcp to the cubic,  $T_{hc}(X)$  and from the cubic to the hcp phase  $T_{ch}(X)$  shown, for instance, in Ref. 11 (Fig. 24). The width of the phase coexistence region in Fig. 12 has been determined from isothermal experiments (squares) and from measurements at constant  $X$  (triangles). The open symbols mark the beginning of the transition, as defined from conductivity,  $M_2$  and  $C_p$  measurements in Figs. 2 and 3 ( $X_B, T_B$ ). Similarly, the closed symbols indicate completion of the transition ( $X_E, T_E$ ). To avoid overcrowding, we have not shown the results of previous investigations, presented in Fig. 11 of Ref. 16. However, our line formed by the open symbols that define the beginning of the transition is in good agreement with previous research. The width for heating through the transition is 0.1–0.2 K, while along isotherms coexistence is maintained over  $\Delta X \approx 3$ –4%. This width could possibly be caused by an inhomogeneity in  $X$  of the order of  $\sim 3\%$  throughout the sample over the concentration range we have investigated. It is not clear how such a large inhomogeneity can arise, but we can make some observations.

First, the transition starts abruptly and also has a well-defined ending, as shown by the various parameters we have measured. Hence, the factors causing the width appear to be different from those that produce the predicted smeared transition in Fig. 4(d) of Ref. 18. The predicted<sup>18</sup> rounding was based on local fluctuations. These would occur as a result of competition between the free-energy change from fluctuations in concentration and the free energy of producing the interface between the two thermodynamic phases. However, the nature of the transition—whether or not it could be crystallographic—was not determined.<sup>18</sup> In solid  $H_2$ , the order-disorder transition drives the  $T_{ch}$  transition, which com-

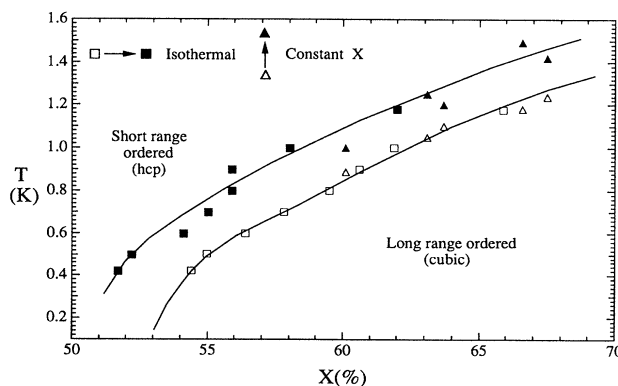


FIG. 12. Phase diagram for the transition from the orientationally ordered to the disordered (or short-range ordered) phase. Open symbols: transition beginning, (shown as  $X_B$  or  $T_B$  in Figs. 3, 4, and 5). Solid symbols: transitions ends ( $X_E$  and  $T_E$ ). The solid lines are drawn as a guide to the eye through the solid and open symbols.

plicates the problem. However, in D<sub>2</sub>, the cubic-to-hcp change can be quenched by repeated thermal cycling, as mentioned before, and, hence, we believe that the crystallographic transition is not a major source in the order-disorder transition broadening.

We note that in their x-ray diffraction studies of Ar<sub>1-X</sub>(N<sub>2</sub>)<sub>X</sub> solid solutions, Klee and Knorr<sup>31</sup> have observed a coexistence region for the cubic-hcp transition. The orientational order-disorder phase change—at least in pure N<sub>2</sub>—is located at a temperature between the martensitic  $T_{hc}$  and  $T_{ch}$  transitions. For pure N<sub>2</sub>, the transition was very sharp, but it broadened with the addition of Ar. Here again, the beginning of the transition was quite well defined, but the end was more smeared. The authors did not consider fluctuations in the composition as the broadening factor but noted that the behavior they observed is characteristic of an athermal martensitic transition.

Second, quantum diffusion-induced clustering of the *o*-H<sub>2</sub> particles producing a departure from the random distribution is probably not the mechanism producing the transition width. The reason for this assertion is that a similar phase coexistence region exists for solid D<sub>2</sub> (see Fig. 11), where the rate of quantum diffusion is much smaller than in H<sub>2</sub>.

Third, if the coexistence of the two phases is produced by a departure from random distribution in *o*-H<sub>2</sub>, then the width should become narrow as  $X \rightarrow 1$ . It would, therefore, be very interesting to extend the measurements to higher concentrations that require enriched *o*-H<sub>2</sub> samples. Investigations have shown that rotational order-disorder transitions in pure compounds such as CH<sub>4</sub> and CD<sub>4</sub> can be extremely sharp,<sup>32</sup> just as that for N<sub>2</sub>.<sup>31</sup>

## V. SUMMARY

We have investigated the thermal conductivity in the orientationally ordered phase and near the order-disorder transition. Simultaneously NMR line-shape and thermal relaxation measurements were carried out, from which qualitative information on the second moment and on the specific heat could be obtained, particularly near the transition. Measurements were conducted along isotherms and versus temperature, where  $X$  changed with time due to ortho-para conversion.

The principal results are as follows.

(1) In the ordered phase, the conductivity is larger than in the disordered one, increasing roughly exponentially with  $X$ . Extrapolation to  $X = 1$  suggests that the conductivity will be as large as for pure *p*-H<sub>2</sub>. The reason for the conductivity enhancement is the diminished inelastic scattering of phonons by excitations of both nearest neighbor *p*-H<sub>2</sub> pairs or clusters and of *o*-H<sub>2</sub>. For  $X \rightarrow 1$ , the *o*-H<sub>2</sub> libron-energy gap becomes much larger than  $k_B T$ , and the inelastic scattering vanishes.

It would be highly desirable to carry out measurements of  $\kappa$  with ortho-enriched H<sub>2</sub>, not available to us at present. This would avoid the long extrapolation up from  $X = 0.70$  to get information on almost pure ortho-H<sub>2</sub>. Furthermore, it would be most valuable if conduc-

tivity on enriched para-D<sub>2</sub> could be carried out, as this would test the influence of stabilizing the cubic phase on  $\kappa$ . Isotherm measurements with D<sub>2</sub> would be much more time consuming than for H<sub>2</sub>, since the para-ortho conversion rate is much lower than in H<sub>2</sub>.

(2) The thermal conductivity in the cubic-ordered phase gave evidence of anisotropy. We believe this not to be an intrinsic property of the cubic state, where anisotropy should vanish. Rather, we attribute the observation to the fact that the sample is an inhomogeneous medium including both cubic crystallites and hcp domain walls.

(3) During the order-to-disorder transition, there is significant width in  $T$ - $X$  space, where ordered and disordered phases coexist. The sharp beginning and end of this region is to be contrasted to a smearing of the transition that would arise from a randomness in the concentration. It would be interesting to consider the aspects of nucleation dynamics to explain the nature of the observed coexistence region. The width of the transition reflects inhomogeneities in  $X$  of 3–4%. We do not understand the origin of these large inhomogeneities.

(4) Various features of properties are different depending on whether the transition moves along an isotherm or as a function of  $T$ . One of the most distinctive is that of  $C_p$  that shows two maxima along isotherms versus one maximum as a function of  $T$  at high enough  $X$  and  $T$ . This might reflect different equilibrium conditions during the measurements. In isothermal measurements, these conditions are much better, allowing more precise data.

(5) Finally, there are unexplained signatures in the thermal conductivity in the hcp phase for  $X \leq 0.52$  for several samples that have previously undergone an order-disorder transition at higher concentrations  $X \geq 0.52$ . These signatures are sharp peaks in the region 1.3–1.4 K.

*Note added in proof.* (1) Silvera and Jochemsen<sup>33</sup> have instigated via far-infrared spectroscopy the H<sub>2</sub> order-disorder transition along an isotherm for  $X = 0.885$  (their Fig. 3). The transition width is  $X_B - X_E \approx 0.025$ , not much smaller than at lower  $X$  (see our Fig. 12). Hence, if the width due to the inhomogeneity in  $X$  is to disappear as  $X \rightarrow 1$ , this has to happen very close to  $X = 1$ . (2) Further experiments with a different conductivity cell, using a crystal-growth technique different to that used before, gave results in agreement with those of our first cell. The experiments were extended to a temperature as low as 0.2 K, limited by the temperature gradient generated inside the sample by the ortho-para conversion heat. Extrapolation of the data of Fig. 12 to  $T = 0$  gave  $X_B = 53.5 \pm 0.5\%$  and  $X_E = 50.5 \pm 0.5\%$ .

## ACKNOWLEDGMENTS

This research was supported by National Science Foundation (NSF) Low Temperature Physics Grant No. DMR 88-20479. The authors acknowledge comments and helpful suggestions on this paper by S. Washburn, A. B. Harris, and C. Jayaprakash, as well as stimulating conversations with R. O. Simmons. We also acknowledge two perceptive remarks on our work by M. S. Conradi.

- <sup>1</sup>R. W. Hill and B. Schneidmeyer, *Z. Phys. Chem. N.F.* **16**, 257 (1958).
- <sup>2</sup>R. G. Bohn and C. F. Mate, *Phys. Rev. B* **2**, 2121 (1970).
- <sup>3</sup>C. L. Reynolds, Jr. and A. C. Anderson, *Phys. Rev. B* **14**, 4114 (1976); **15**, 5466 (1977).
- <sup>4</sup>J. E. Huebler and R. G. Bohn, *Phys. Rev. B* **17**, 1991 (1978).
- <sup>5</sup>J. H. Constable and J. R. Gaines, *Phys. Rev. B* **8**, 3966 (1973).
- <sup>6</sup>M. Calkins and H. Meyer, *J. Low Temp. Phys.* **57**, 265 (1984).
- <sup>7</sup>B. Ya Gorodilov, I. N. Krupskii, V. G. Manzhelii, and O. A. Korolyuk, *Fiz. Nizk. Temp.* **12**, 326 (1986) [*Sov. J. Low Temp. Phys.* **12**, 186 (1986)].
- <sup>8</sup>X. Li, D. Clarkson, and H. Meyer, *J. Low Temp. Phys.* **78**, 335 (1990).
- <sup>9</sup>O. Ebner and C. C. Sung, *Phys. Rev. B* **2**, 2115 (1970).
- <sup>10</sup>V. B. Kokshenev, *J. Low Temp. Phys.* **20**, 373 (1975).
- <sup>11</sup>For a review, see I. F. Silvera, *Rev. Mod. Phys.* **52**, 393 (1980); J. Van Kranendonk, *Solid Hydrogen* (Plenum, New York, 1983).
- <sup>12</sup>R. Wanner, H. Meyer, and R. L. Mills, *J. Low Temp. Phys.* **13**, 337 (1973).
- <sup>13</sup>L. I. Amstutz, H. Meyer, S. M. Myers, and D. C. Rorer, *Phys. Rev.* **181**, 589 (1969).
- <sup>14</sup>J. V. Gates, P. R. Granfors, B. A. Fraass, and R. O. Simmons, *Phys. Rev. B* **19**, 3667 (1979).
- <sup>15</sup>A. B. Harris, S. Washburn, and H. Meyer, *J. Low Temp. Phys.* **50**, 151 (1983).
- <sup>16</sup>R. Banke, M. Calkins, and H. Meyer, *J. Low Temp. Phys.* **61**, 193 (1985).
- <sup>17</sup>A. Onuki, *J. Phys. Soc. Jpn.* **58**, 3065 (1989); **58**, 3069 (1989), and references therein.
- <sup>18</sup>Y. Imry and M. Wortis, *Phys. Rev. B* **19**, 3580 (1979).
- <sup>19</sup>D. T. Lawson and H. A. Fairbank, *J. Low Temp. Phys.* **11**, 363 (1973).
- <sup>20</sup>G. A. Armstrong, A. A. Helmy, and A. S. Greenberg, *Phys. Rev. B* **20**, 1061 (1979).
- <sup>21</sup>J. F. Jarvis, H. Meyer, and D. Ramm, *Phys. Rev.* **178**, 1461 (1969).
- <sup>22</sup>Y. Suemune, *J. Phys. Soc. Jpn.* **22**, 735 (1967).
- <sup>23</sup>T. A. Scott, *Phys. Rep.* **27C**, 89 (1976).
- <sup>24</sup>H. M. Roder, *Cryogenics* **2**, 302 (1965); L. A. Koloskova, I. N. Krupskii, V. G. Manzhelii, and B. Ya Gorodilov, *Fiz. Tverd. Tela (Leningrad)* **15**, 1913 (1973) [*Sov. Phys. Solid State* **15**, 1278 (1973)].
- <sup>25</sup>W. N. Hardy, I. F. Silvera, and J. P. McTague, *Phys. Rev. B* **12**, 753 (1970).
- <sup>26</sup>C. F. Coll III and A. B. Harris, *Phys. Rev. B* **4**, 2781 (1970).
- <sup>27</sup>S. Washburn, M. Calkins, H. Meyer, and A. B. Harris, *J. Low Temp. Phys.* **49**, 101 (1982).
- <sup>28</sup>M. Calkins, R. Banke, X. Li, and H. Meyer, *J. Low Temp. Phys.* **65**, 185 (1986).
- <sup>29</sup>R. Banke, X. Li, D. Clarkson, and H. Meyer, *J. Low Temp. Phys.* **72**, 99 (1988).
- <sup>30</sup>G. Ahlers and W. H. Orttung, *Phys. Rev.* **133**, A1642 (1964).
- <sup>31</sup>H. Klee and K. Knorr, *Phys. Rev. B* **42**, 3152 (1990).
- <sup>32</sup>R. O. Simmons, *Trans. Am. Crystallogr. Assoc.* **17**, 17 (1981).
- <sup>33</sup>I. F. Silvera and R. Jochemsen, *Phys. Rev. Lett.* **43**, 377 (1979).